GRANT NGR-21-002-040

U. Md.

NASA PROGRESS REPORT [redacted]

MICROWAVE MEASUREMENT OF PROTEIN HYDRATION AND OF END GROUP CHARGE ACTIVITY

REPORTING PERIOD: 2/1/66 to 7/30/66

ABSTRACT

A research program investigating the dielectric absorption of microwave frequencies for specific neuroproteins is in progress. It is expected that this investigation will yield information on the water of hydration of the macromolecule and on specific end group anisotropic activity which will be of value in both structural and physiological interpretation. The microwave cavity for this dielectric measurement has now been completed and is illustrated. Features of the instrument are discussed. The design and construction of a controlled-environment chamber is reported, with graphic information showing the time-voltage relationships which plateau the chamber to a variety of final temperatures.

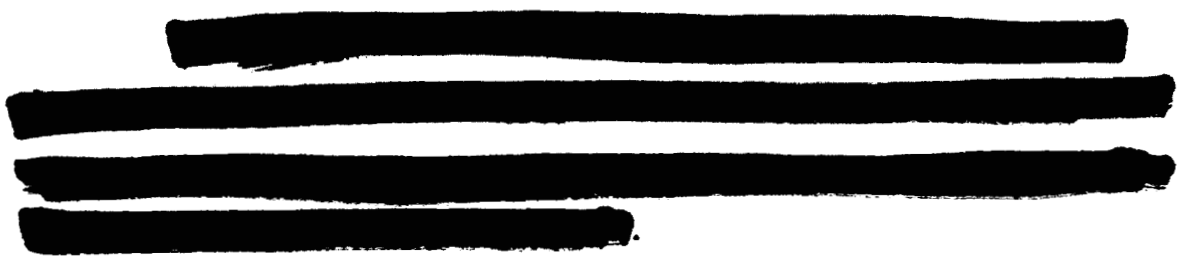

MICROWAVE CAVITY

Final design of the basic microwave cavity assembly was completed prior to our last report, with a reduction of the design included (1). The cavity was constructed during the current reporting period. J. B. Rodgers, an experienced microwave machinist at the Johns Hopkins University, completed the basic assembly, [redacted] This instrument is illustrated in Figures 3 and 4. As finally completed, the cavity features some improvements not shown in the design. The dovetail section was fabricated as a unit with the heavy brass stabilization jacket around the waveguide. This gives improved rigidity and allows the use of a single longitudinal parting line to assemble the entire housing around the waveguide core in just two sections. The two assemblies were mounted by using locating pins, machine screws, and sweat-soldering.

Nylon set screws are used to adjust out any residual play in the fit of the transverse carriage to the dovetail section, and positive locking is accomplished by tightening a set screw against the opposed bearing plate. The coupling iris is made integral with the waveguide flange. Its 0.005 in. thickness maintained across the front guide section promises a low order of cavity perturbation. The matching stub assembly was constructed in our own laboratory. The shorting stub from a surplus Hewlett-Packard Detector Mount, Model No. X-485, was cleaned ultrasonically and screwed to a concentric knob and mounting bracket. As shown in Figure 6-b, the bracket swivels to permit mounting on any surface. The complete cavity assembly as illustrated in Figure 6-a, is similar to that used by Dr. P.O. Vogelhut at the University of California (2), but the detailed differences mentioned are expected to improve its structural stiffness.

CONTROLLED-ENVIRONMENT CHAMBER

The controlled-environment chanber was designed to provide both electrical and thermal isolation and to provide temperature control within 0.01°C for the duration of the cavity sweep. Its design is diagrammed in Figure 2, but the dimension scale should be ignored, as the figure is a reduction from the original drawing. It was built in the laboratory from wood and pressed board, 1/4 in. and 1/8 in. thick, with "Vermiculite" packed into the insulation spaces. Two layers of aluminum foil provide electrostatic shielding and reduce radiation heat losses. An access door allows tuning and other adjustments to be made while the cavity is in place near the floor of the chamber. Exterior views of the chamber are found in Figure 9.

Opposite the access door is located the mount for a heating coil with ample capacity to increase the interior temperature to 60°C. Initial measurements of dielectric absorption will be made under constant heater voltage conditions from a regulated source. Figure 1 graphs voltage vs. final temperature for a series of thermal equilibria of the chamber. From this information we will select the voltage required for the desired measurement temperature. Interior temperature will be monitored at a copper-constantin junction by a Leeds & Northrop slide wire potentiometer, with a Weston standard cell and a reference junction at 0°C. However, the thermistor-controlled amplifier, for which a schematic was included in our previous report (3), is currently under construction and will be incorporated in the chamber when completed. The SCR circuit utilizes phase-controlled switching to regulate the heater voltage steplessly and thus avoids temperature cycling. A Veco small bead thermistor, No. 38C2, is

located next to the cavity itself, and its resistance becomes one arm in a bridge circuit which controls the heater amplifier gain, as in Figure 7. A variable resistance in one arm of this bridge is adjusted to match the resistance of the thermistor at the low end of the temperature range to be covered. Provision has been made for the installation of a small Rotron air-circulating fan next to the heating coil. If differential temperature layers result in convection currents which cause short-term thermal instability at the cavity, controlled air circulation will be used to provide a uniform chamber temperature.

ULTRASTABLE MICROWAVE OSCILLATOR

A proposed arrangement to use microwave equipment at the Johns Hopkins University for our initial measurements unfortunately could not be implemented. As a result, we have been forced to undertake our own microwave instrumentation at the outset, and there have been unfortunate delays in the acquisition of much of this equipment, largely traceable to the suppliers. These changed circumstances have retarded the measurement schedule of the experimental program outlined in the last report, and the effort which would have been expended in control measurements has been diverted to hardware.

However, an X-band generator, the LFE No. 814 A-X-21 Ultrastable Oscillator, has been acquired on an evaluation loan through the courtesy of the manufacturer and of the Jay Company, Falls Church, Virginia. With the typical high-Q cavity characteristic found at microwave frequencies, we expect a loaded sample cavity Q of the order of 3×10^3, which represents a half-power bandwidth of 3×10^6 Hz at 10^{10} Hz, where

$$Q = \frac{f_o}{(f_1 - f_2)} \tag{1}$$

for $Q >> 10$ (4). The use of this oscillator, with the slow sweep rates implicit in the electrical parameters for a stabilized-mode sweep, requires a mechanical drive system such as used by Vogelhut. On the LFE, one 360° rotation of the expanded frequency scale represents a sweep of

9.655 GHz - 9.405 GHz = 245 MHz

Thus, at 1.45°/MHz, Δf of 20 MHz represents a 29° rotation. At 9.450 GHz, 20 MHz represents a maximum Δf in the stabilized mode of operation. Choosing this frequency band and a total sweep duration of 5 minutes, the rotational dial speed becomes 3°/min. for a constant sweep rate. This speed may be provided conveniently by the "hour hand" drive of a synchronous clock motor, and thus a moderately crude mechanical system will entirely suffice to evaluate the instrument and to provide control measurement data. The drive is currently under construction and will provide voltage for the X-drive of a Moseley X-Y Recorder from a mechanical linkage.

A step-up gear from the motor is coupled to a 20-turn Helipot. The potentiometer acts as a voltage divider across a DC source, providing a proportional voltage to the recorder X-input. As the LFE provides a high degree of sweep linearity for small dial displacements, this signal is proportional to the arc travel of the sweeper dial and, therefore, to f. The cavity characteristic may thus be displayed graphically by patching into the Y-input the voltage square-law detected from the cavity reflection. Relative Q amplitude and the half-power frequency shifts characterizing a sample solution may be taken directly from the graph.

We plan to use a 15 GHz counter for calibration of frequency, the Systron Donner No. 1037/1292 Digital Counter, and counter application may be extended to direct cavity Q measurement by using differentiating circuit techniques at the half-power or inflection points. Mr. Thomas M. Bray of the Johns Hopkins University has suggested circuit applications which would measure the amplitude and frequency of Q maxima, and these systems are being investigated.

MEASUREMENTS

A sample measurement program is outlined below and will be undertaken upon the completion of instrumentation necessarily more extensive than was originally planned. Control materials will be measured first, to determine the agreement of the extrapolated static dielectric constant and of the estimated water of hydration with the results from other investigations of these rather well-studied soltions. We expect to have completed the instrumentation and to have made these measurements before the next reporting period. Concurrently, we will have undertaken the extraction of neuroprotein from nerve menbrane, nerve, and neurons, as described in our first report (5), and this will be measured, as were the controls, to estimate bound water by relative dielectric absorption. The techniques necessary for the extraction of protein from the lipids of the surrounding membrane are exacting. However, they involve well understood biochemical routines and there is every reason to expect that we will have useable fractions of perhaps 80% homogenous material when the control measurements are completed. Our first series with the nerve proteins will then directly follow the establishment of control standards.

Initial measurements will be made on distilled water only, at four temperatures: 25°C, 30°C, 37.5°C, and 40°C. Using sterile distilled water to avoid bacterial decomposition, 2% solutions of bovine albumin, hores haemoglobin, globulin, and gelatin will be measured at the above temperatures and the results examined for their agreement with those of Buchanon, et. al., (6) and of Schoenborn, et. al (7). The cavity will be charged with the sample by locating a transverse glass capillary tube in the 1/8 in. saddle bore shown in figure 5 and through the slotted line axis. Sample tubes have been made with an interior diameter of 0.060 in. and a length of 2 in., enclosing a central volume of 0.00565 $in.^3$, or 0.0912 $cm.^3$. The liquid will be drawn into the tubes by connecting a partial vacuum at one end, and the sample will then be sealed off by inserting 0.060 in. Teflon plugs.

Upon inquiry, Mr. Barney of the Research Laboratory at Corning Glassworks, has suggested the following low-loss glasses which could be used at microwave frequencies:

Corning Allow Code #	Material	Trade Name	Loss Tangent at 10 GHz
7070			0.0021
0120			0.0063
7900	fused silica	Vicor	0.0009
9606	glass ceramic		0.0005

Initial measurements will be made using "Vicor", which Corning has courteously agreed to provide at no charge.

THEORETICAL SYNOPSIS

The Haggis, et. al., technique for determining bound water from relative measurements of the extrapolated dielectric constant (8), is predicated on the wide separation of the relaxation peaks for water, which relaxes at λ_m = 1.56 cm. at 25°C (9), and for the much larger protein molecule, which relaxes at wavelengths which are greater by 5 to 6 orders of magnitude. Though anomalous dispersion distributes this phenomenon over a broad frequency base, any relaxation overlap is small, and the protein appears as a prolate elliptic spheroid in the Buchanon, et. al., model (10).

The model of spheroidal cavities of low ε suspended at random in a dielectric of high ε has been treated theoretically by Palder (11), Lewin (12), Fricke (13), et. al. Where β is a parameter depending on the oblate-prolate axial ration, the decrement, δ, is given by

$$(2) \qquad \delta = \beta \left[(\varepsilon_w - \varepsilon_{\infty p})^v + (\varepsilon_w - \varepsilon_{\infty w})^w \right] \times 10^{-2}$$

v is the partial specific volume of protein, and w is the weight of water irrotationally bound to 1 gm. of protein. The subscripts are the dielectric constants of water, w, for protein, p, and at high frequency, ∞. Assuming the linear dependence of ε_s, the static dielectric constant, on C, the protein concentration in gm/ml solution

$$(3) \qquad \varepsilon_s = \varepsilon_w - \delta C.$$

For relative measurements, the expanded treatment of the complex dielectric

constant given by Onsager (14) and Kirkwood (15), promises no increase in accuracy over the original relationship given by Debye (16), which relates the static and high frequency dielectric constants in the expression from von Hippel (17),

$$(4) \qquad \tan \delta = \frac{\varepsilon'}{\varepsilon''} = \frac{(\varepsilon_s' - \varepsilon_\infty') \, w \, \tau_e}{\varepsilon_s' + \varepsilon_w' \, w^2 \, \tau_e^2}$$

where tan δ is the loss tangent and

$$(5) \qquad \tau_e = \frac{\tau \, (\varepsilon_s' + 2)}{\varepsilon_\infty' + 2}$$

At an $\vec{E}_{max}$ sample location, Birnbaum and Franeau (18) relate the complex dielectric constant, ε^*, given by

$$(6) \qquad \varepsilon^* = \varepsilon' - j\varepsilon'',$$

to the sample volume, v, cavity volume, V, and to half-power frequency and Q in the relationships,

$$(7) \qquad \frac{f_1 - f_2}{f_2} = 2 \, (\, \varepsilon' - 1 \,) \, \frac{v}{V}$$

$$(8) \qquad \frac{1}{Q_2} - \frac{1}{Q_1} = 4 \, \varepsilon'' \, \frac{v}{V}$$

Vogelhut (19) modifies (7) and (8) to give

$$(9) \qquad \Delta \varepsilon' = \varepsilon'_w - \varepsilon'_s = \frac{2C}{f_o} (f_s - f_w)$$

and

$$(10) \qquad \Delta \varepsilon'' = \varepsilon''_w - \varepsilon''_s = C \left(\frac{1}{Q_s} - \frac{1}{Q_w} \right.$$

The relative changes in ε' and ε'' for the volume enclosed by the sample capillary tube are associated with shifts in the resonant frequency, f, for the sample solution, s, for water, w, and with f_o as the resonant frequency of the empty cavity. The cavity constant, C, derives from the volume of the empty cavity, V, from the volume of the dielectric sample material, v, and from the correction, A, for the location of the sample relative to $\vec{E}_{max}$.

Given a polarization of $\vec{\mu}$ debye, Onsager (20) develops a static-field expression for this polarization in terms of Avogadro's number, N, the gas constant, k, the permittivity of free space, ε_o, and the absolute temperature, T. The importance of a constant thermal environment is borne out in its exponential relationship to $\vec{\mu}$,

$$(11) \qquad \vec{\mu}^2 = \frac{9\varepsilon_o}{N} kT \; \frac{(2\varepsilon'_s + \varepsilon'_\infty) (\varepsilon'_s - \varepsilon'_\infty)}{\varepsilon'_s (\varepsilon'_\infty + 2)^2}$$

Onsager avoids the well-known Mosetti catastrophe (21) in which the polarization becomes indeterminate for a unity value of a polarizability term in the denominator of a quotient, and he considers dipole interaction between polar molecules and their isotropic surroundings. Kirkwood (22) is currently attempting the microscopic equations for the

local fields of individual dielectrics. It is clear that the mathematics for other than relative dielectric absorption phenomena will have to be founded in this later theory.

We do not propose to undertake the mathematics of later molecular dielectric theory at this time. Our data for neuroproteins will be fitted to the Debye equations, and irrotationally-bound water will be determined quantitatively from cavity absorption by using the Vogelhut relationships. However, the extension of our measurements program into the anisotropic effects produced on microwave absorption by molecular orientation in the solute molecule (23) will ultimately require that the limitations of the Debye theory be dealt with, and it is hoped that the application of later molecular dielectric ideas will provide pre-Doctoral material for a graduate consultant in mathematics.

BIBLIOGRAPHY

1. Grenell, R.G., NASA Progress Report, 3/30/66
2. Vogelhut, P.O., Nature, 203, 1169 (1964)
3. Grenell, R.G., op.cit.
4. "Handbook Of Microwave Measurements", Vol. I, Polytech. Inst. Brooklyn, 1955
5. Grenell, R.G., NASA Proposal, 1/30/65
6. Buchanon, T.J., Haggis, G.E., Hasted, J.B., Robinson, B.G., Proc Roy Soc Lon, 213, 379 (1952)
7. Schoenborn, B.P., Featherstone, R.M., Vogelhut, P.O., Susskind, C., Nature, 202, 695 (1964)
8. Haggis, G.E., Buchanon, T.J., Hasted, J.B., Nature, 167, 607 (1951)
9. Smyth, C.P., "Dielectric Behavior and Structure", New York, 1955,p. 129
10. Buchanon, T.J., op. cit.
11. Palder, Physica, 12, 257 (1946)
12. Lewin, J. Instor Elect Engrs, 94, 65 (1947)
13. Fricke, Phys Rev, 24, 575 (1924)
14. Onsager, L., J. Am Chem Soc, 58, 1486 (1936)
15. Kirkwood, J.G., J. Chem Phys, 7, 911 (1939)
16. Debye, P., "Polar Molecules", Ch V, New York, 1929
17. von Hippel, A.R., "Dielectrics and Waves", New York, 1954, p. 176
18. Birnbaum, G., Franeau, J., J App Phys, 20, 817 (1949)
19. Vogelhut, P.O., op. cit.
20. Bottcher, C.J.F., "Theory Of Electric Polarization", New York, 1952
21. Onsager, L., op. cit.
22. von Hippel, A.R., op. cit., p. 181
23. Grenell, R.G., (1), op. cit.

Fig 1. [illegible] temperature plotted cavity number.

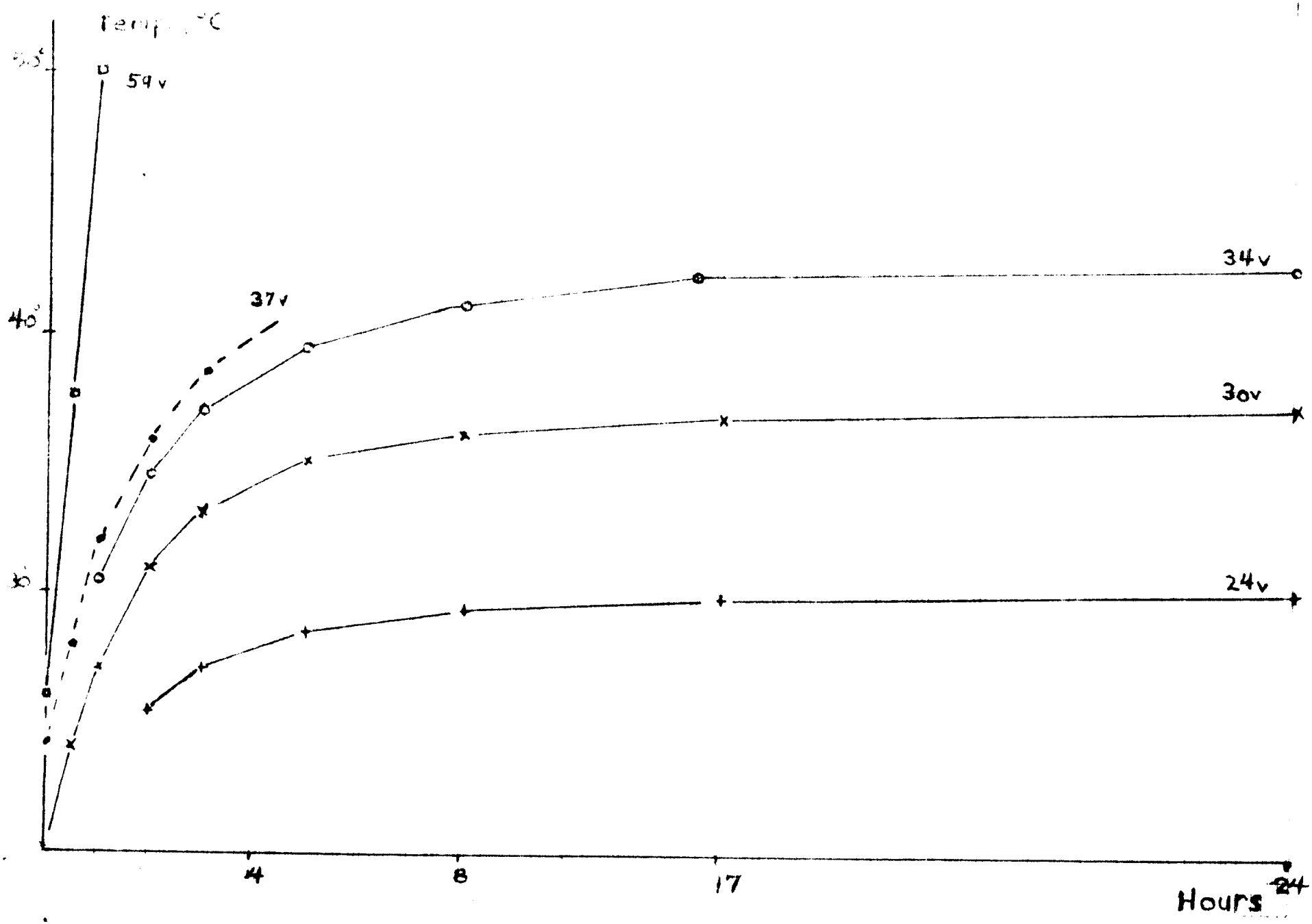

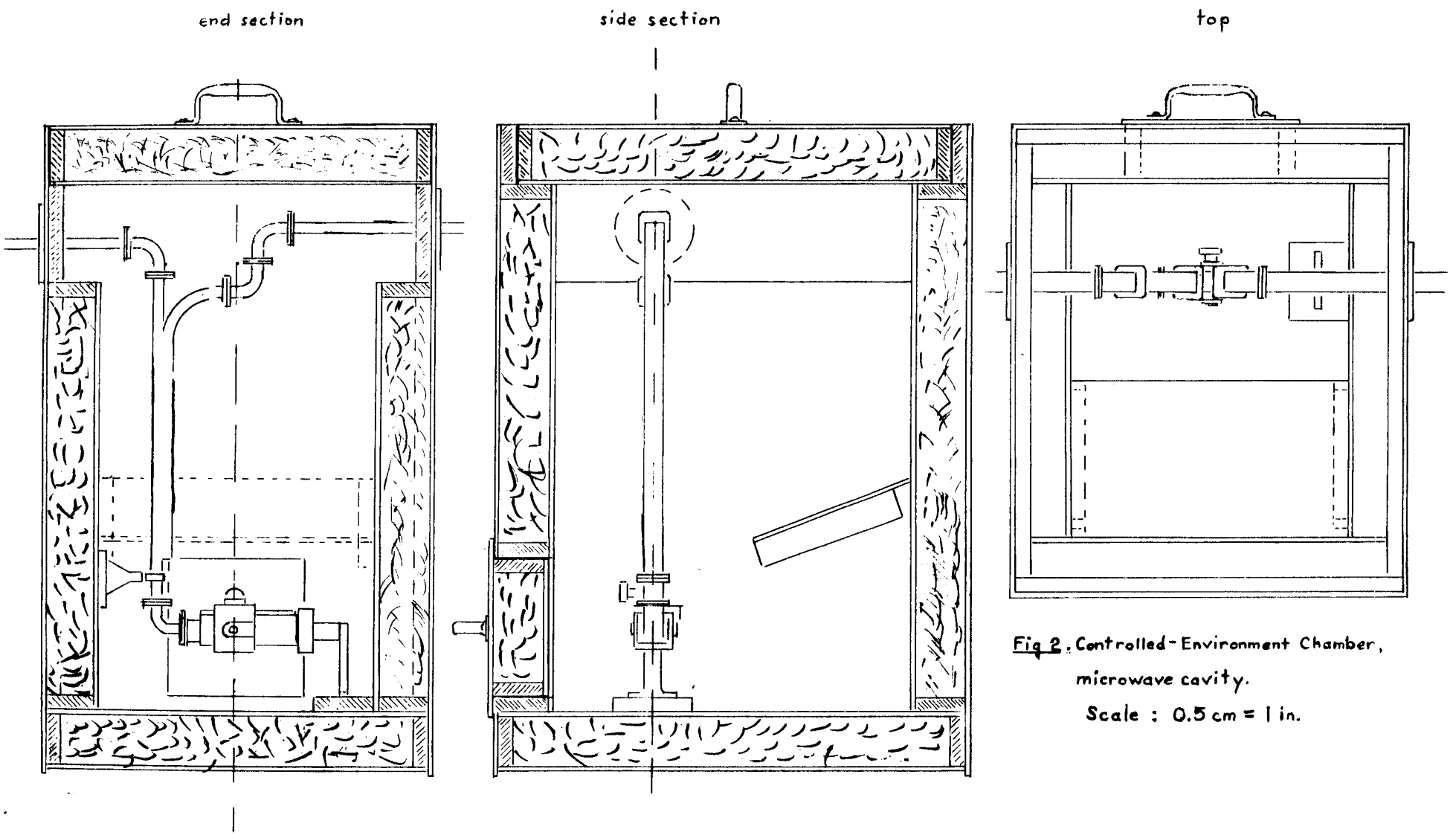

Fig 2. Controlled-Environment Chamber, microwave cavity.
Scale : 0.5 cm = 1 in.

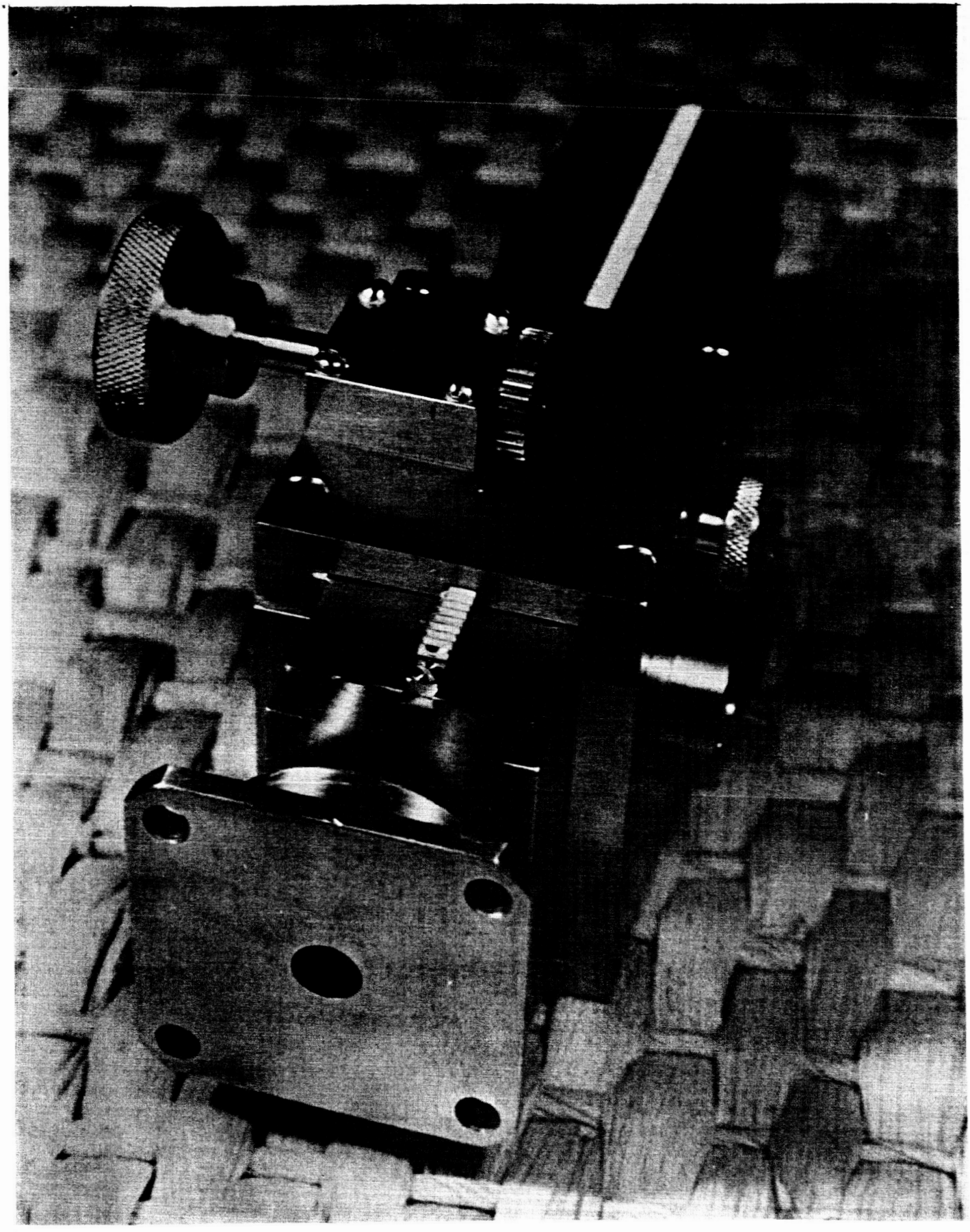

Fig. 3. Microwave cavity from coupling flange end.

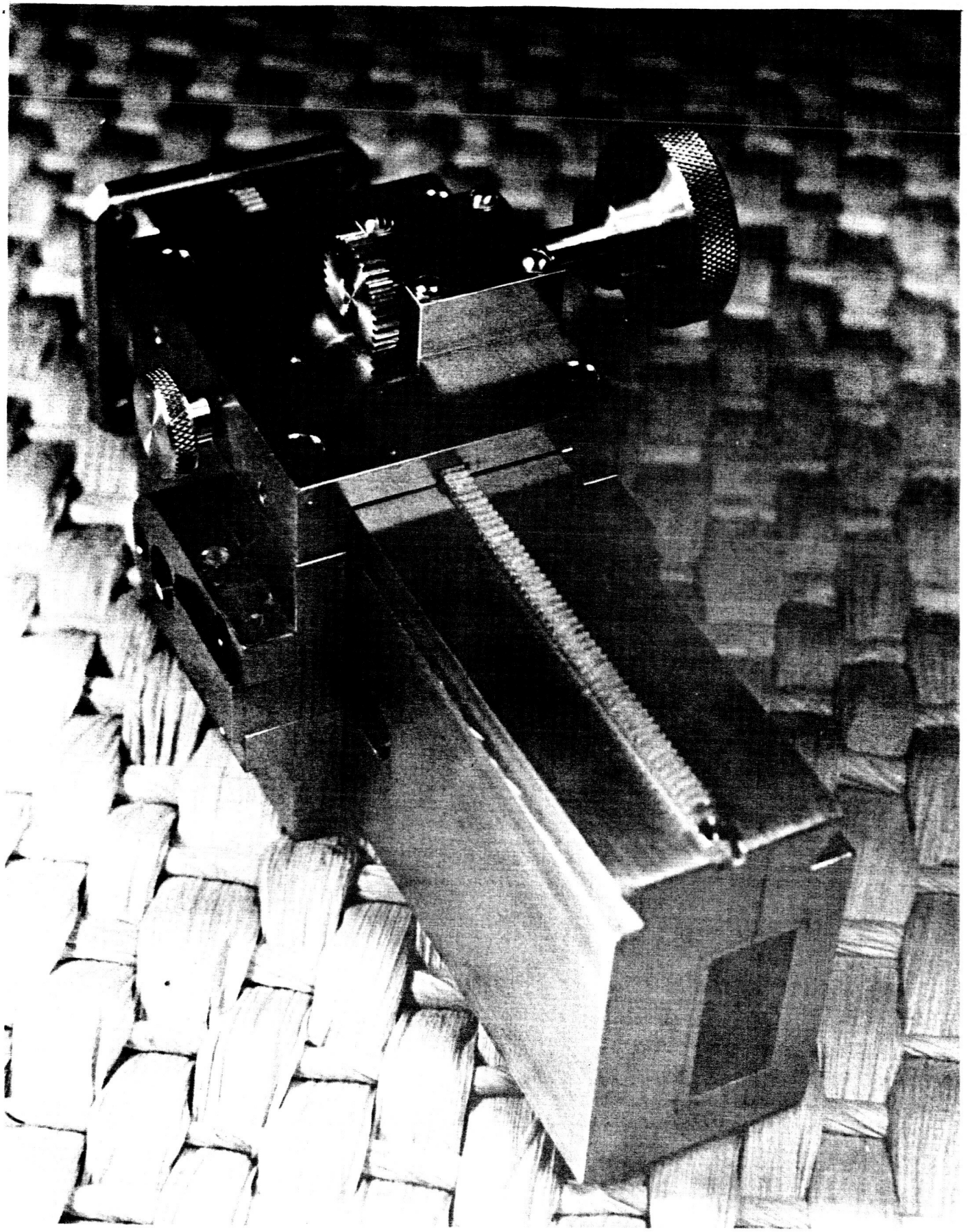

Fig. 4. Cavity from reflection end, without matching stub.

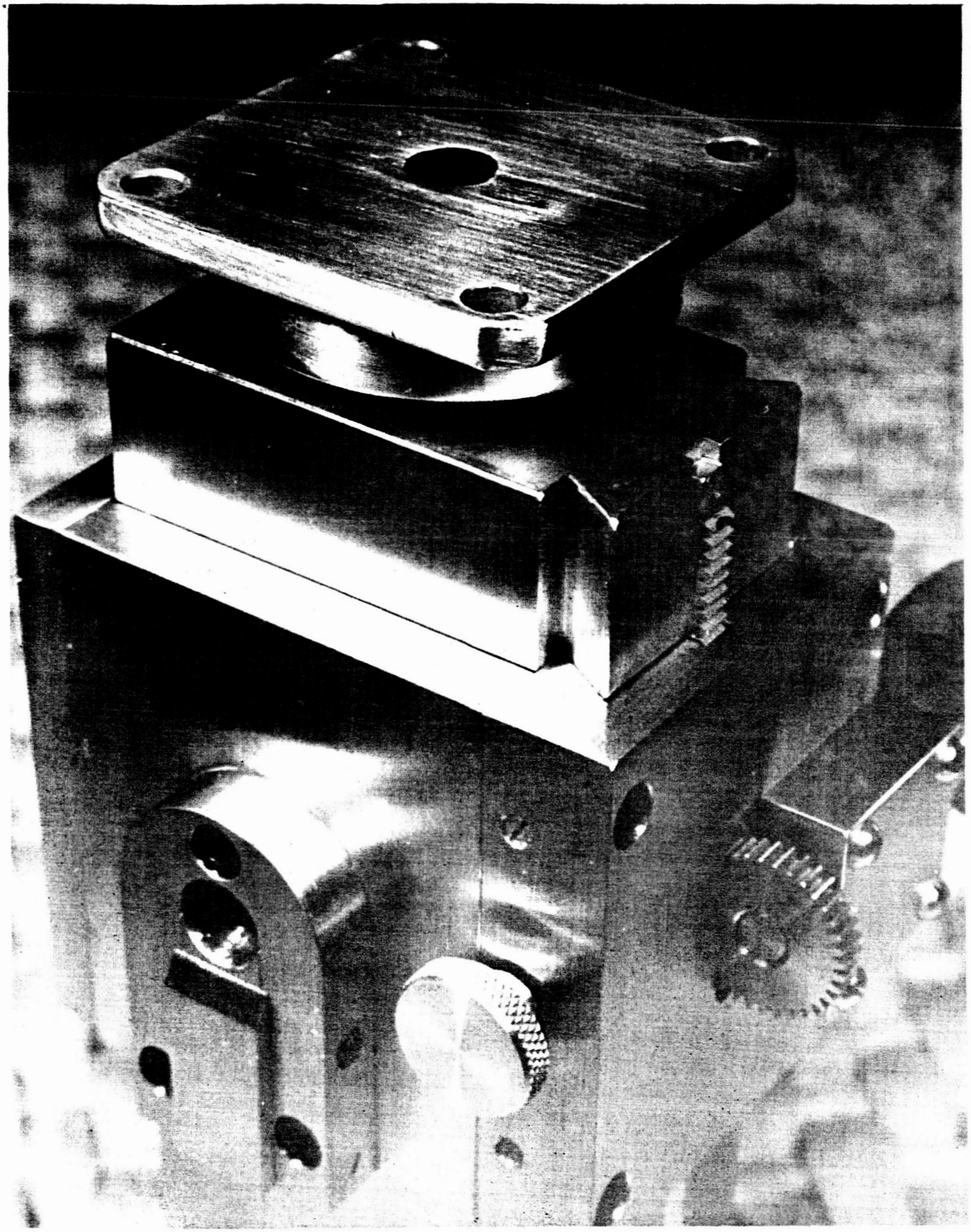

Fig. 5. Close-up showing saddle dovetail and clamping screw.

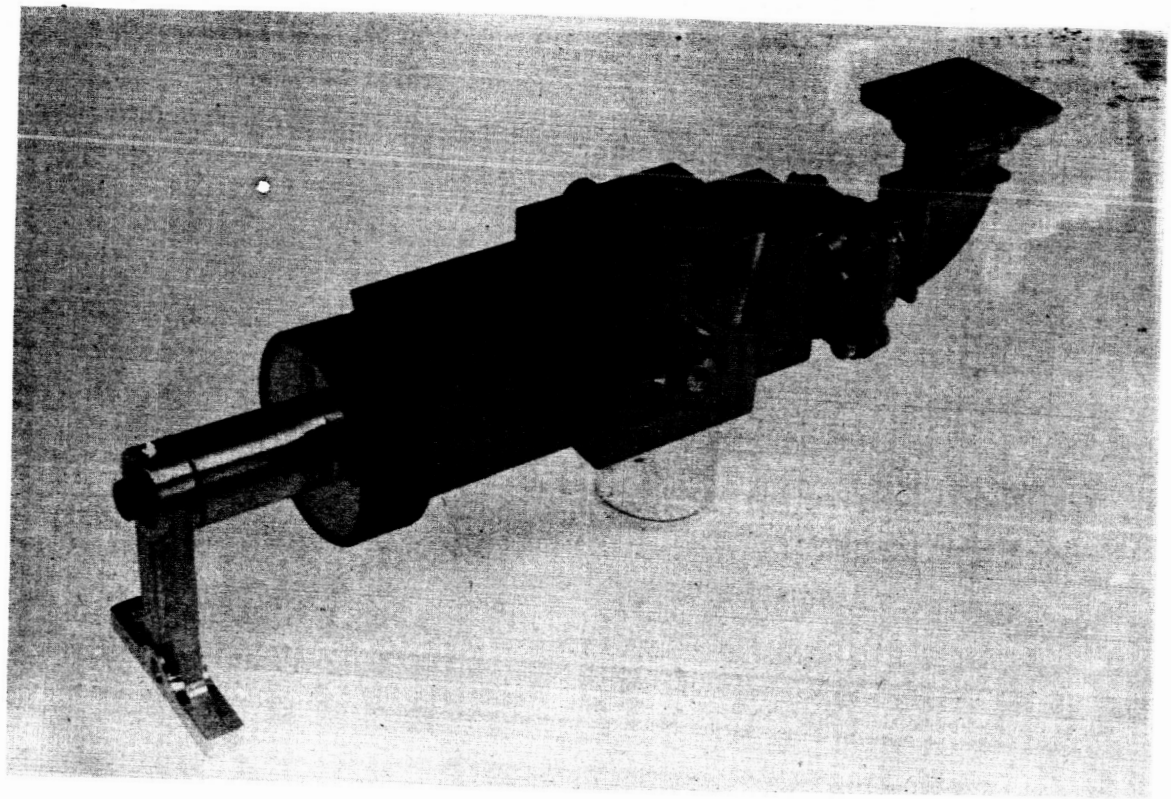

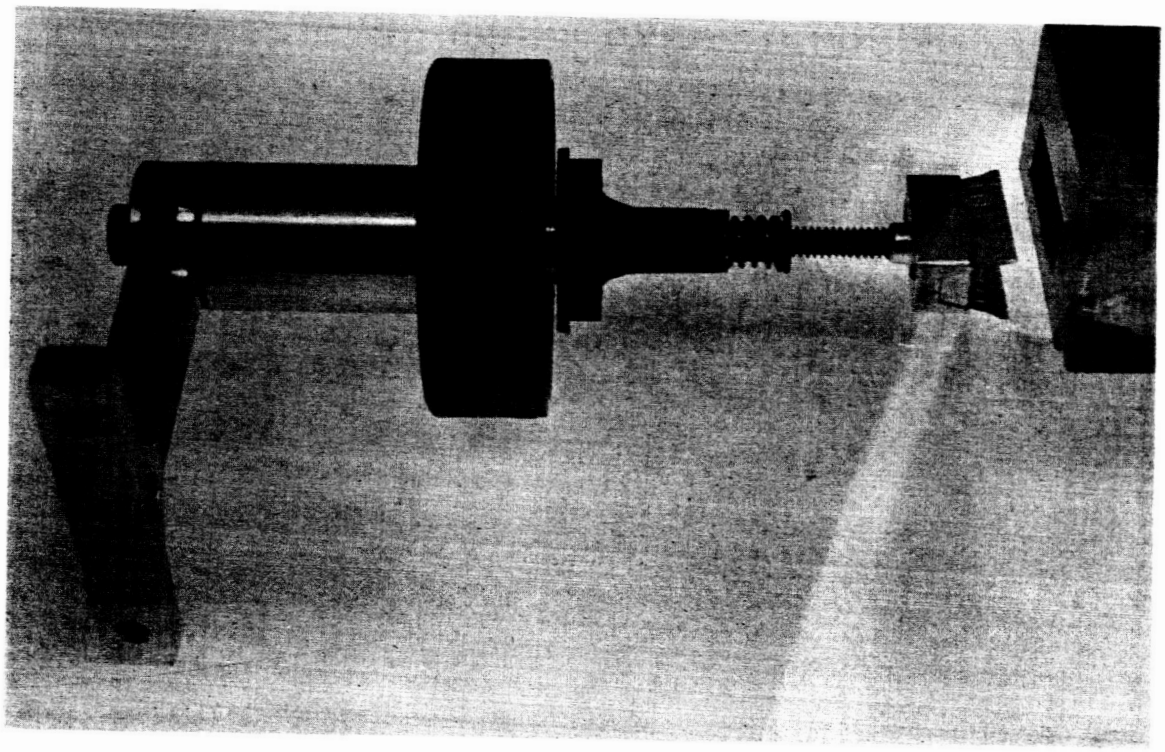

Fig. 6. Top. Complete cavity assembly.
Bottom. Matching stub, with adjustment knob and mounting bracket.

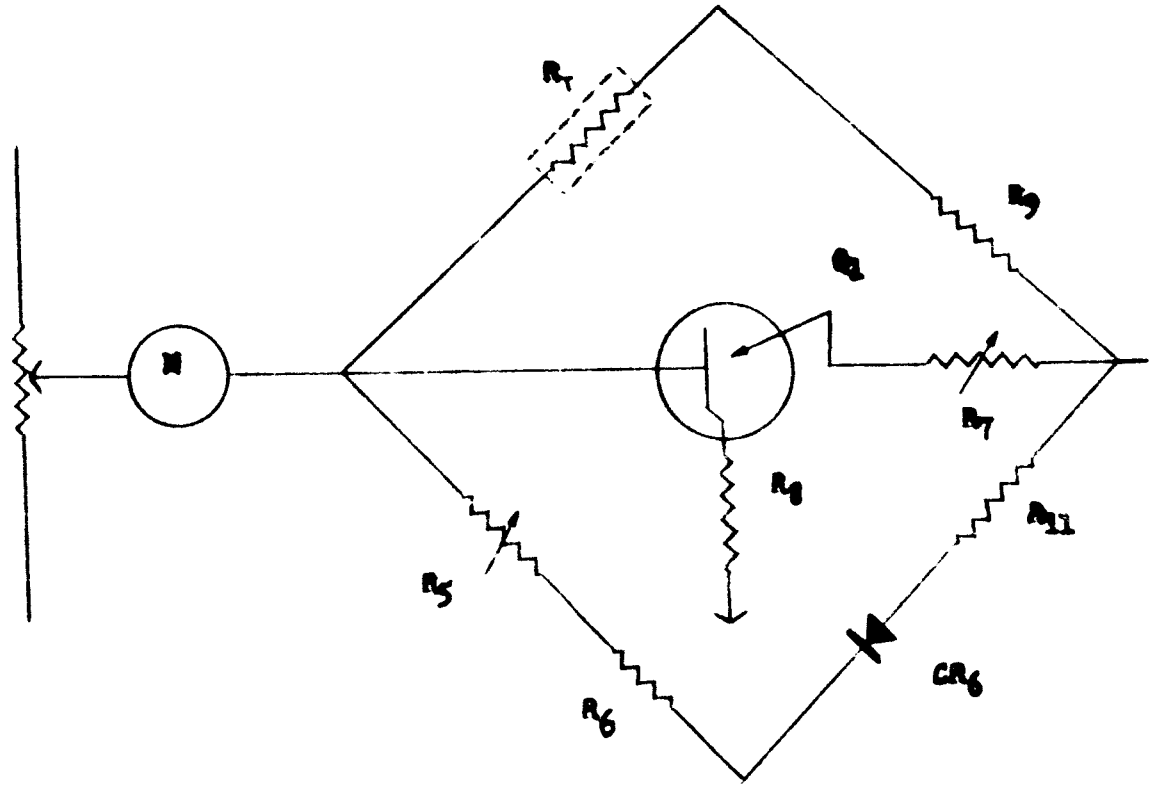

Fig. 7. Temperature Control Bridge, [illegible] Thermistor.

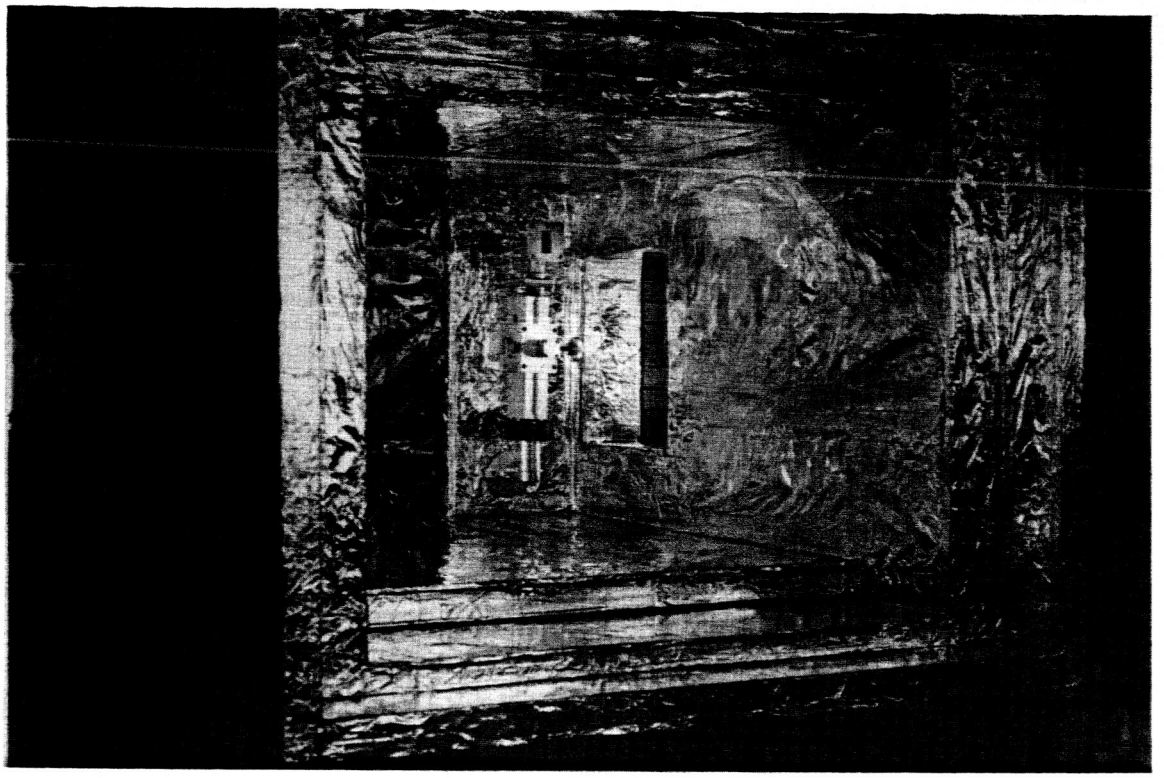

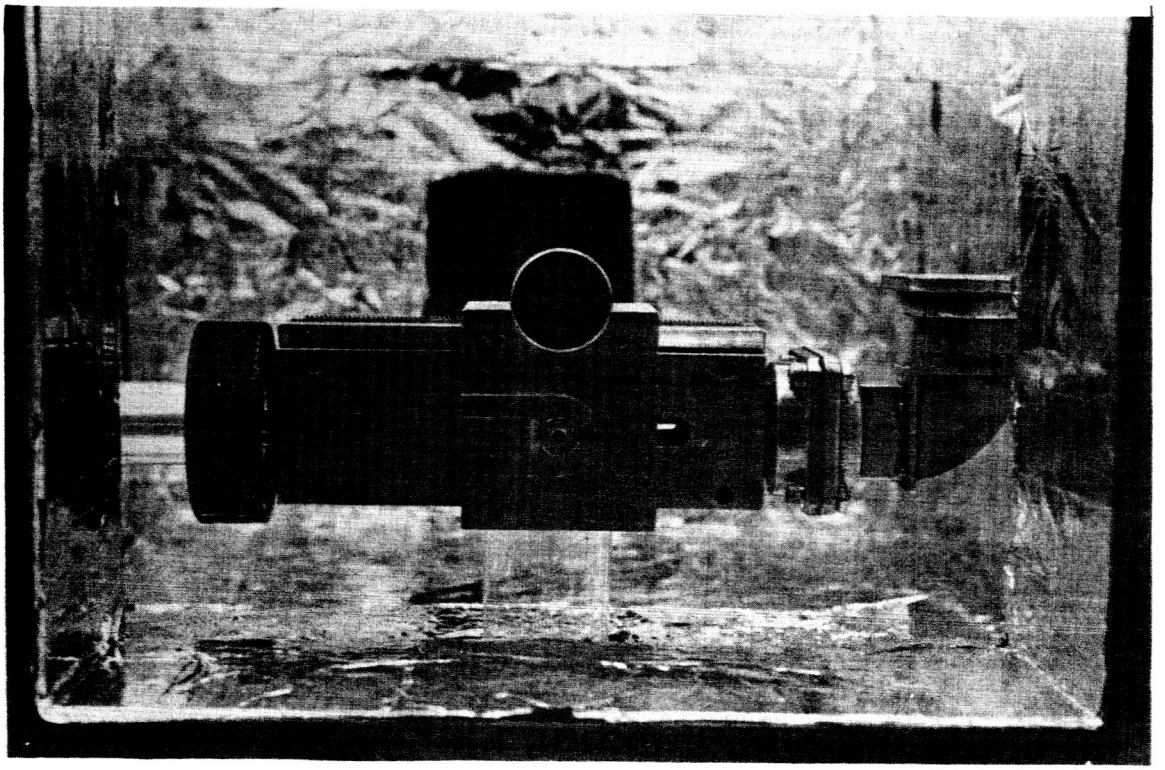

Fig. 8. Top. Chamber viewed from top door.

Bottom. Cavity assembly in place in controlled-environment chamber. Viewed from access door.

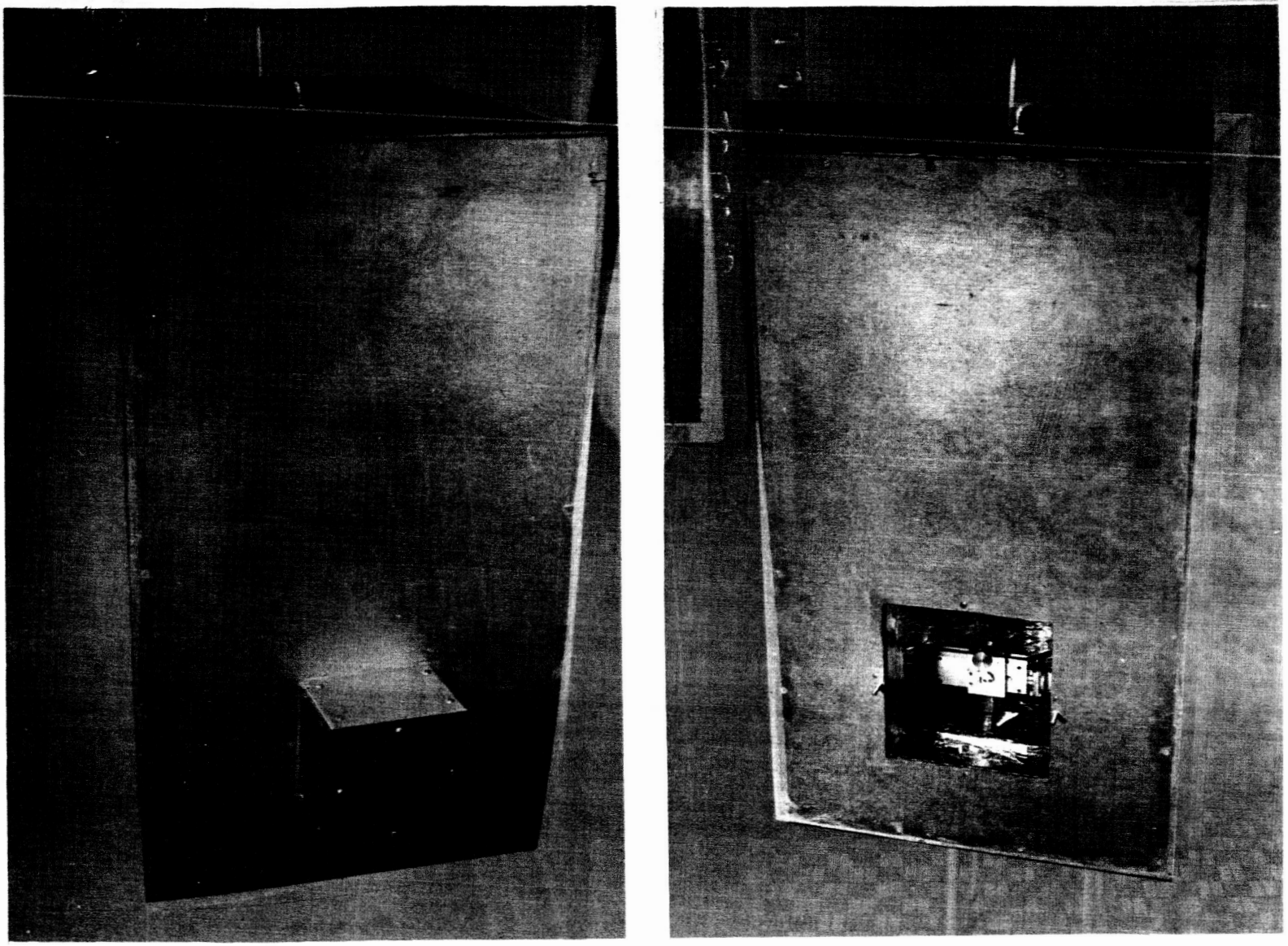

Fig. 9. Exterior views of chamber, from cavity and heater sides.